Progress In Electromagnetics Research C, Vol. 161, 66–75, 2025

PIER C

(Received 17 July 2025, Accepted 15 October 2025, Scheduled 28 October 2025)

SADEA-Tuned Broadband Circularly Polarized Metasurface-Inspired Monopole Antenna for Next-Generation Wireless Applications

Iltapawar T. Laxman[1], Harikrishna Paik[1], Bikash R. Behera[1,*], and Mohammed H. Alsharif[2]

[1]*Department of Electronics and Communication Engineering, School of Electrical and Communication Vel Tech Rangarajan Dr. Sagunthala R&D Institute of Science and Technology Chennai, Tamil Nadu 600062, India*
[2]*Department of AI Convergence Electronic Engineering, Sejong University Seoul, Seoul 05006, South Korea*

ABSTRACT: In this investigation, a broad circularly polarized high-gain SADEA-tuned quasi-TM_{30}-mode excited metasurface antenna at sub-6 GHz 5G band is shown. A linearly polarized (LP) monopole antenna in stage-1 with conventional partial ground is proposed. Then, in stage-2, a stair-cased partial ground plane is transformed to witness circular polarization (CP), an expanded part of stage-1. In stage-3 for next-generation wireless applications, the main objective is to improve CP gain, impedance (10-dB BW), and axial bandwidths (3-dB BW), which will make it a good candidate for RF energy harvesting systems, a potential feature for next-generation wireless application. In this case, the application of a metasurface layer is an important step, significantly optimized by using AI-tuned SADEA method. The SADEA-tuned metasurface layer at 45 mm right above the $\lambda/4$ monopole radiator is integrated as a multi-layered structure. Finally, it is fabricated on a low-cost FR-4 substrate with thickness of 1.6 mm and offers a measured 116.3% 10-dB BW, 20.98% 3-dB BW, CP gain $^{\text{peak}} > 7.5$ dBic, and antenna efficiency $> 85\%$ in the desired band of operation. With the introduction of SADEA optimization method not only the complexity was reduced while designing the metasurface layer, but simultaneously to the best of author's knowledge, this is the first time such type of approach is followed towards the design of circularly polarized metasurface antenna for next-generation wireless applications.

1. INTRODUCTION

There are high performance expectations for data throughput, reliability, coverage, spectrum, as well as energy efficiency, connectivity density, and latency in the era of next-generation wireless communication systems, especially in the sub-6 GHz spectrum allotted to the 5G. Enhancing the capabilities of wireless systems and radio frequency (RF) front-ends, which are crucial in determining the directions of wireless communications in the future, has received attention in an effort to satisfy these demanding criteria [1, 2]. So, this development promotes new paradigms like energy-autonomous devices and makes it easier to expand the functionality of wireless systems. Given recent advancements, research on the deployment of RF energy harvesting (RF-EH) systems that use ambient RF signals, specifically in the sub-6 GHz 5G bands, is now becoming increasingly necessary. RF-EH offers a viable strategy for lowering operating expenses and maintenance frequency since it captures and transforms electromagnetic (EM) energy into electrical power that may be used. Since effective RF front-ends consistently interface with EM waves coming from multiple directions, their design is crucial in this context. So, regardless of the direction of the incoming wave & the receiving antenna, circular polarization (CP) has drawn interest as the best method for enhancing signal reception and impedance matching. RF front-ends with low profiles, wide impedance bandwidth, high radiation efficiency, and steady radiation pattern are required for the accurate receptions of mobile communication signals in 1–7 GHz. They also need to adhere to the emission limits established by the Federal Communications Commission (FCC) [3, 4] for their better results. As a consequence, there is a requirement for the single antenna element that possesses attributes, mostly the capability of CP. So, the techniques in the likes of vias [5] and metasurfaces (MTSs) [6–12] are utilized in order to accomplish the design of CP antenna. On the other hand, when it comes to the need for effective polarization system, one of the important instances is to attain broadband CP. The particular kind of analogy and the existing antenna designs' comparison of performance trade-offs were not specified in [5–12] as they continue to be significant. It is especially true when the deployment of MTS is not defined through artificial intelligence (AI) in the prospect of reducing the complexity of implementing multi-layered structure. Thus, the the optimization of MTS is needed to antenna for its augmentation in bandwidth and gain, which has not been seen yet in the literature.

Surrogate-assisted differential evolution algorithm (SADEA) [13, 14] is employed with the objective of optimizing the structural parameters of MTS towards enhancing performance, by considering the trade-offs, especially the enhanced 3-dB bandwidth and 3-dB gain in the sub-6 GHz 5G band, which has not yet been reported in the literature.

* Corresponding author: Bikash Ranjan Behera (drbikash@veltech.edu.in).

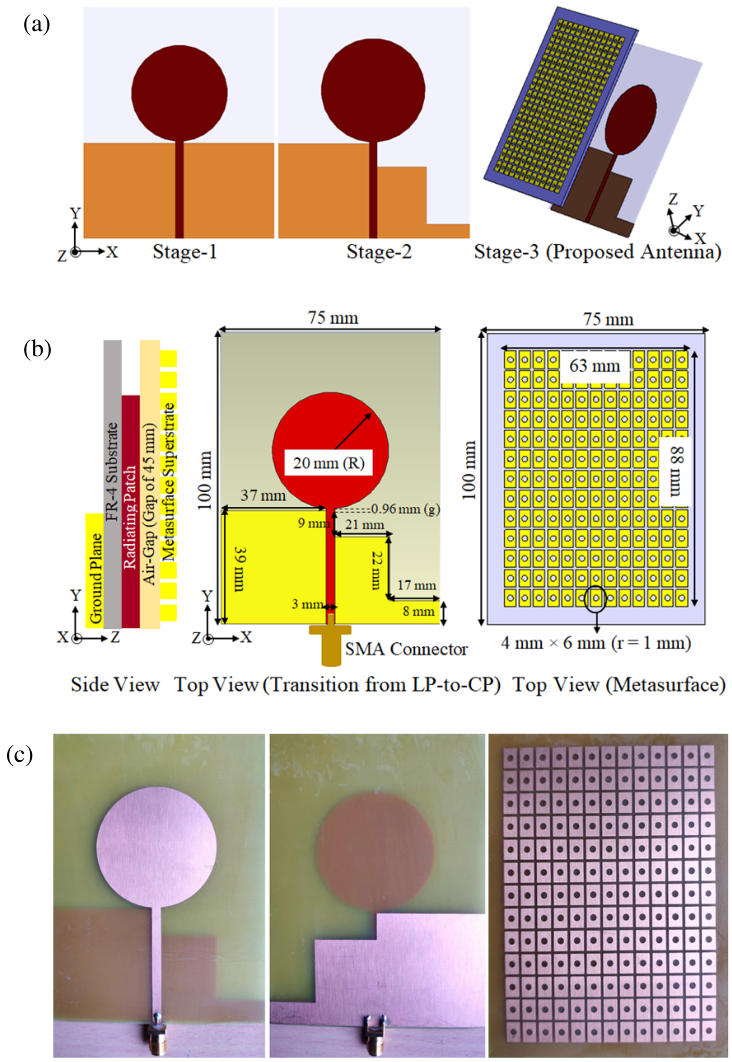

FIGURE 1. (a)–(c) Evolution stages and schematics of a proposed SADEA-tuned CP MTS antenna along with its fabricated prototype using PCB prototyping mechanism.

Thus, the inclusion of stair-cased partial ground plane and the SADEA-driven MTS layer of uniform symmetrically positioned unit cells makes it possible to achieve broadened CP bandwidth and gain with broadside-directed pattern in sub-6 GHz 5G bands, which was earlier a major roadblock in this particular field-of-interest. So, this article shows that a SADEA-tuned circularly polarized MTS-inspired monopole antenna is proposed, and it witnesses a good performance, attains broadened 3-dB bandwidth of $>$ 20% and CP gain $^{\text{avg.}}$ of $>$ 6.5 dBic with better front-to-back ratio (FBR) at sub-6 GHz 5G band considered to be ideal from an application perspective.

2. ANTENNA DESIGN AND EXECUTION OF SADEA OPTIMIZATION METHOD

A circular-shape printed monopole antenna (CSPMA) is shown in Figures 1(a)–(c). Its operational features are dependent on the lowest resonant frequencies (f_L). In a sub-6 GHz 5G band, the CSMPA lowest resonant frequency is at 1 GHz (stage-1), which is visualized by using Computer Simulation Technology (CST) microwave studio EM solver, and it makes use of the empirical formula in Equation (1) for consideration towards the design of a $\lambda/4$ monopole antenna:

$$f_L = \frac{7.2}{2.34R + g}\,\text{GHz} \tag{1}$$

From above, in Equation (1), f_L represents the lowest resonant frequency, R the radius of the structure, and g the gap that exists between the radiating patch and a partial ground plane, which contributes towards the improvement of impedance matching. Based on the existing literature, monopole antennas are more familiar for ultra-wideband (UWB) in broader senses because of the intrinsic features that they demonstrate, but the adoption of their creditability is not widespread in the frequency spanning up to 7 GHz. Also, one of its limitations pertains to restricted presence and inability to achieve viability as a result of the existing antenna designs' non-responsive behaviour towards the CP characteristics. Considering the scenario of today's communication systems in a sub-6 GHz 5G band, there is an urgent need for the RF front-ends with strong radiation, high CP antenna gain, and better antenna efficiency (stage-2). The utilization of SADEA-tuned MTS layer offers a vast contribution for attaining broadband CP through the manipulation of focused, strong directional pattern with increased FBR and 3-dB angular beamwidth (stage-3), quite applicable from an application perspective.

Now, we will proceed to elaborate on the phenomena of adding SADEA-tuned MTS layer. We make usage of the MATLAB RF antenna toolbox$^{\text{TM}}$, they have access to the broad number of functions and applications which are utilized for the motive of designing, analyzing, and optimizing the RF components, based on the requirements from application perspective. In our design, the component element mainly consists of uniform unit cells, which are the fundamental constituents of MTSs that have been optimized to extract best possible antenna performance considering the performance trade-offs. By looking into the optimization, it is possible to deduce the outcomes by utilizing discrete 3D forms & arbitrary planar structures governed by parametric equations. Also, they provide a powerful way-out to represent and manipulate the geometric objects, and these objects can be manipulated based on our considerations. Due to the usage of EM solver, it is able to compute the attributes in order to figure out final verifications, in the same way methods of moments (MoM) does, but the matured optimizations allow for the structures to be optimized in the most efficient manner possible, enabled through the utilizations of AI-driven optimization methods, which are applied very rarely in the case of MTS unit cells. So, an approach known as a SADEA is applied to maximize design effectiveness by making use of artificial intelligence. This optimization method, grounded for machine learning and evolutionary computations, leverages AI to find optimal solution in a very effective manner taking into consideration for lesser complexity and exhibition of better performances in terms of attaining the trade-offs. It employs AI to design from the scratch and iteratively improve its designing & mimicking natural evolution for exploring its integration through the design spaces for the final antenna structure. In the context, to draw the attention of the readers, a detailed analogy on the surrogate model assisted differential evolution for antenna synthesis (SADEA) and its implementation is shown in Figures 2(a) and (b).

With the help of SADEA method, the phenomenon of global optimization which makes usage of statistical learning approaches develops the surrogate model. Hence, in the framework of the surrogate model-assisted optimization, it is of quite relevance that the processes applied to make the surrogate modeling optimization in an effective manner. It has included ideas taken from evolutionary search framework that take surrogate models in accordance with the time. In relation to it, differential evolutions (DEs) also known as Gaussian processes (GPs) are employed in the search engine where a SADEA method utilizes the insides of a machine learning process exclusively used for a surrogate modeling [13–15]. To summarize the overall process of AI-tuned SADEA optimization, the following steps can be taken into consideration:

→ **Step-1: Initialization** — Create a population of potential solutions at first, each of which represents a different antenna design parameter with different characteristics.

→ **Step-2: Surrogate Model Training** — A subset of evaluated solutions is utilized to train a surrogate model as the DE process moves on. Thus, based on the values of its parameters, this model learns to forecast how well antenna design parameters would function and put impact on the final performance.

→ **Step-3: Optimization Process** — The surrogate model is used to direct the DE algorithm. So, instead of executing a full simulation for each design parameter, the model predicts its performance, and the DE algorithm is then utilized to select the top dimensions for the next phase of execution before it is integrated in the final design structure.

→ **Step-4: Updating Surrogate** — It is updated with the most recent dimension after a sufficient number of iterations have been tested. As a result, it can get better over the time and make predictions that are more accurate.

→ **Step-5: Termination** — The process of optimization will continue until stopping criterion is satisfied, which could be a predetermined number of iterative generations from the beginning or the discovery of a solution that provides adequate response. In order to optimize the antenna design parameters for better results, SADEA not only minimizes costly simulations but also preserves the resilience of DEs.

$$h_{air\text{-}gap} = 0.76\lambda - h_{sub}\sqrt{\varepsilon_r} \tag{2}$$

As far as the authors are aware, there are very few reports on the usages of the surrogate-assisted differential evolution algorithm (SADEA) to the design of a circularly polarized (CP) metasurface (MTS) antenna. In order to close this gap and improve performance, we report SADEA-based MTS layer optimization in stage-3. Here, the grid-slotted sub-patches, intermediate gaps, and overall MTS dimensions are among the structural changes that are the focus of the optimization. According to stage 2, an MTS superstrate is positioned 45 mm ($h_{air\text{-}gap}$) above the λ/4 CP monopole antenna. Parametric analysis is carried out to assess performance trade-offs prior to finalization. Table 1 provides summary of the findings. Equation (2) presents the corresponding mathematical formulation. Here, the average CP

TABLE 1. Placement of the superstrate in stage-3: Parametric study and its effect on various outcomes.

$h_{air\text{-}gap}$	Impedance Bandwidth	Axial Bandwidth	Antenna Gain $^{\text{Avg.}}$
30 mm	107.3%	--------	--------
35 mm	110.1%	--------	--------
40 mm	112.7%	--------	--------
45 mm	**117.2%**	**21.52%**	**7.1 dBic**
50 mm	119.4%	10.75%	7.15 dBic
55 mm	130.2%	10.68%	7.28 dBic
60 mm	143.8%	--------	--------

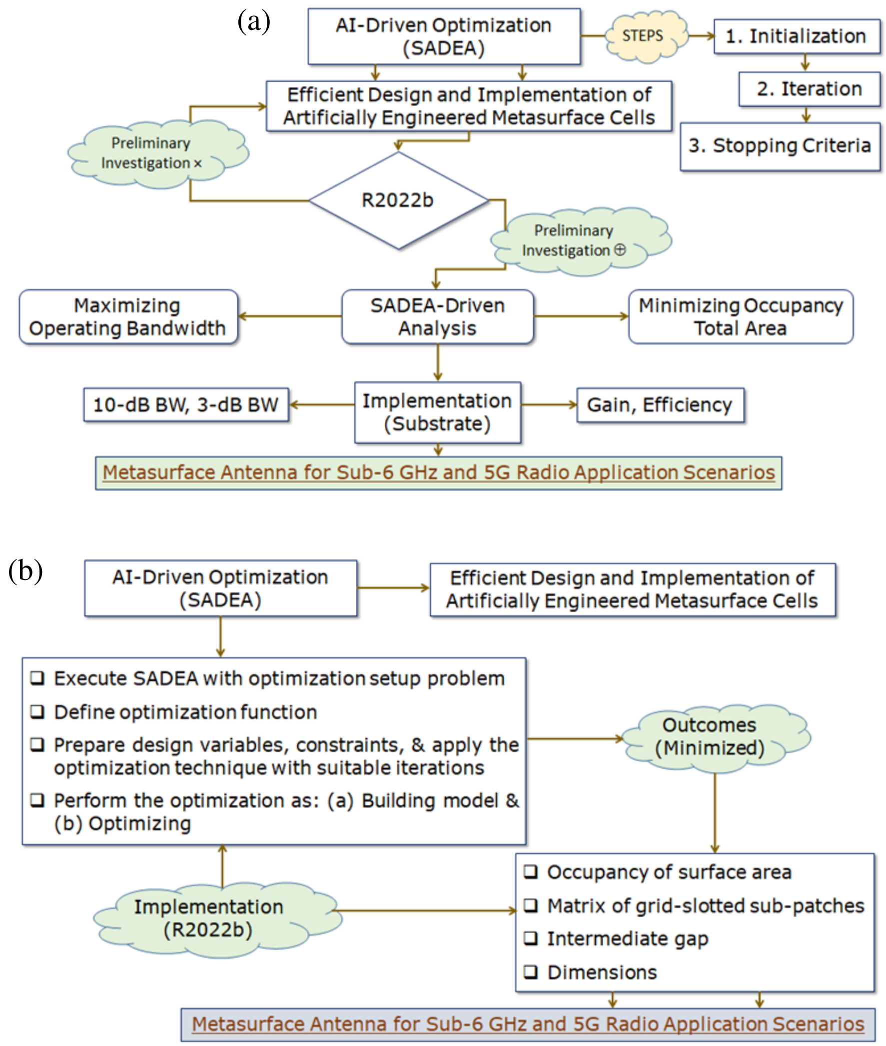

FIGURE 2. (a), (b) Concept and implementation process of SADEA optimization method for the designing of MTS layer.

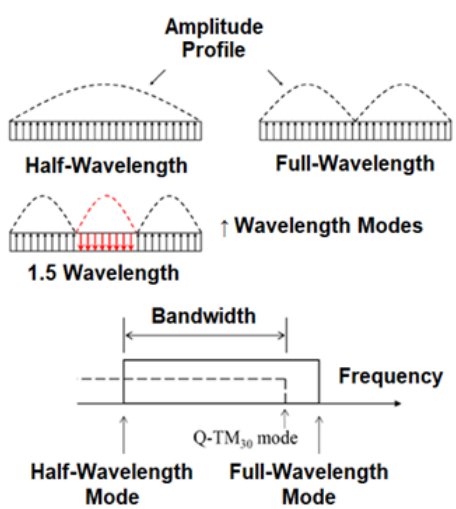

FIGURE 3. Generation of higher-order modes in stage-3 due to the implementation of metasurface layer.

gain increases from 2.38 dBic (stage-2) to 7.1 dBic (stage-3), according to performance study, which translates to a enhancement factor of roughly 2.98. Furthermore, there is a 1.52-fold improvement in the 3-dB axial ratio bandwidth, which rises from 14.1% to 21.52%. These outcomes demonstrate how well SADEA works to optimize MTS structures for improved CP antenna.

Both of these increments are possible due to the implementation of SADEA-tuned MTS layer being present as a top layer. This improvement is significant, as it attains the offsets in terms of CP gain and bandwidth. In the current process, it is observed that the attainment of maximized outcomes in terms of improvement of performances is driven by geometric features. Previously, it is seen that the MTS unit cells focus radiation beam on quasi-TM_{30} modes (i.e., a transition from TM_{10}-to-TM_{30} modes, half-wavelength mode to full-wavelength modes). It is expressed in the form of grid-slotted sub-patches that are the sources of high-orders modes, considering λ. In Figure 3, it is observed that because of the gaps (marked in a red colour) between the grid-slotted sub-patches or MTS unit cells, there is transition of the modes that is related to the improvement of a CP bandwidth to 1.52 times. So, the comparison of various outcomes at different instances is pur-

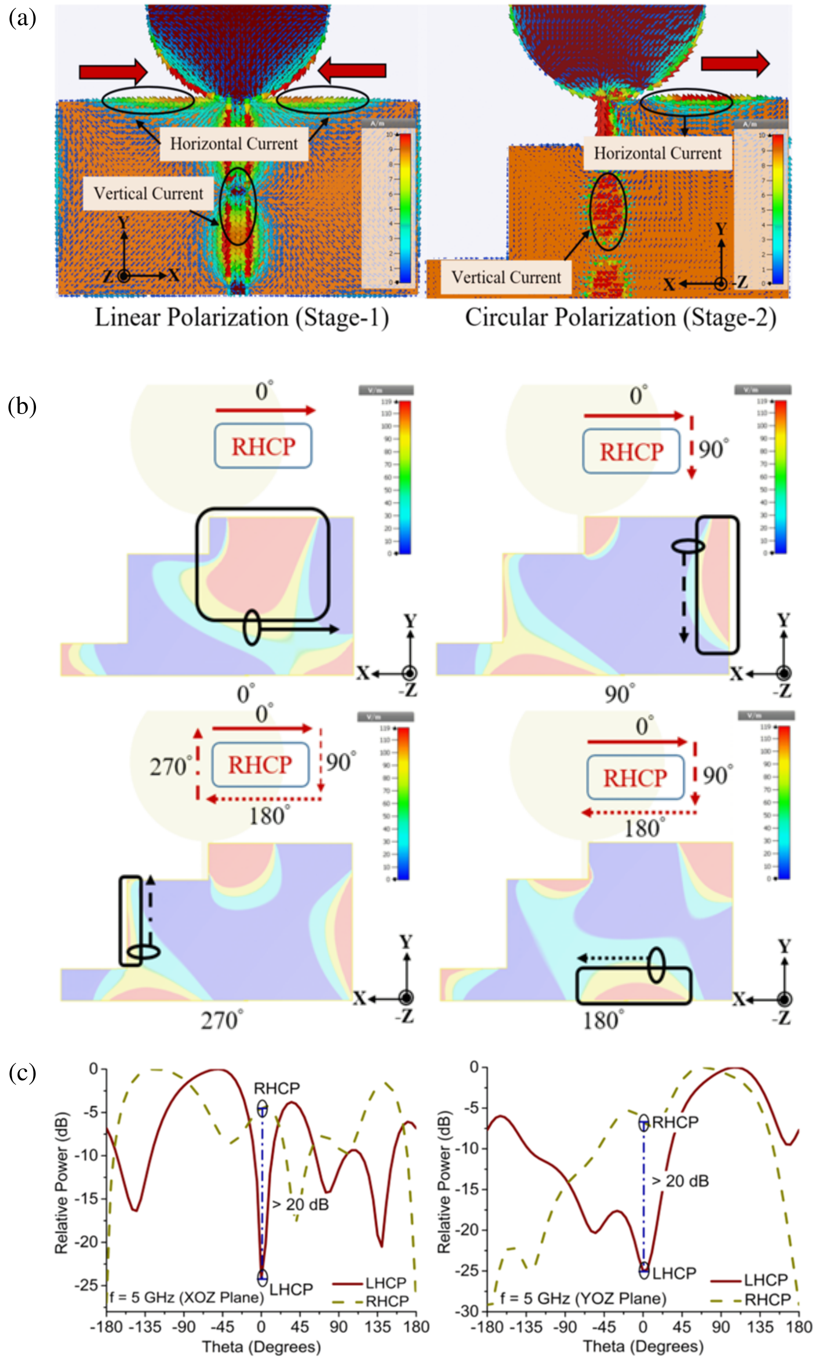

FIGURE 4. Evaluation of CP mechanism at 5 GHz: (a) method-I, (b) method-II, and (c) method-III.

sued in Table 2. In addition to it, there is a direct influence of the suppression of surface wave resonances leading to the efficient far-field radiation pattern at sub-6 GHz 5G bands. Finally, we can give interesting insight that there is a strong connection between physical properties of MTS layer and enhancement of antenna gain nearly to 2.98 times. Since MTS layer can control the phase, amplitude, as well as polarization of the waves, shaping the wave front allows them to guide their radiated energy in more focused directions, improving the directivity of antenna and so its gain simultaneously in a broader manner [16].

3. EVALUATION OF CIRCULAR POLARIZATION CHARACTERISTICS

A comprehension of CP attributes is interpreted in Figures 4(a)–(c). The first and second methods are executed to look at surface current and electric field distributions at sub-6 GHz 5G bands. In Figure 4(a), the vertical and horizontal components indicate that the CP behaviour is present in our case. The second method observes the electric field to figure out the type of CP (i.e., left hand circular polarization (LHCP)/right hand circular polarization (RHCP)). The nature of CP is RHCP as the

TABLE 2. Corresponding outcomes at the various stages of proposed antenna in the sub-6 GHz 5G bands.

Evolution	Polarization	Impedance Bandwidth	Axial Bandwidth	Antenna Gain $^{Avg.}$	Performance
Stage-1	LP	142.8%	×	×	×
Stage-2	CP	144.8%	14.1%	2.35 dBic	3-dB BW √ 3-dB Gain ×
Stage-3	**CP**	**117.2%**	**21.52%**	**7.1 dBic**	**3-dB BW ↑** **3-dB Gain ↑**

TABLE 3. A comparison of stage-3 with the reported works in [5–12] (**Trade-offs:** Impedance Bandwidth $> 115\%$, Axial Bandwidth $> 20.5\%$, CP Antenna Gain $^{Avg.}$ > 6.5 dBic, CP Antenna Gain ^{Peak} > 7.5 dBic, are all considered, where × means not attained and √ means attained).

References	Impedance Bandwidth	Axial Bandwidth	CP Antenna Gain		Complexity
			Average	Peak	
[5]	×	×	×	×	↑
[6]	×	×	×	×	↑
[7]	×	×	×	×	↑
[8]	×	×	×	×	↑
[9]	×	×	×	×	↑
[10]	×	×	×	×	↑
[11]	×	×	×	×	↑
[12]	×	×	×	×	↑
Stage-1	√	×	×	×	↑
Stage-2	√	×	×	×	↑
Proposed Work (Stage-3)	√	√	√	√	↓

electric fields are moving in a clockwise around the direction of propagation in which the field components rotate at 90° with each other. Thus, when the phase changes from 0° to 90°, it can be seen that the pattern of the electric field changes perpendicularly to the phase and resembles a clockwise movement pattern. Concurrently, the strength of electric fields still exhibits a similar pattern as they move from 90° to 360° in the clockwise direction keeping in constant to the direction of propagations (i.e., $+z$-direction). Here, researchers often describe these features by using a right-hand thumb rule and represent it with plane wave equation [16] shown in Equation (3). Considering this mathematical intuition, Figure 4(b) highlights the attributes of CP as an RHCP. Further, the third method identifies the type of CPs through the examination of radiation patterns at sub-6 GHz 5G bands. Figure 4(c) presents that the RHCP is stronger than LHCP. A CP gain of 1.735 dBic at LHCP and 2.26 dBic at RHCP is obtained at 5 GHz (stage-2). Therefore, this approach makes it possible to appreciate the features of CP components in terms of a left-handed circular polarization (LHCP) or right-handed circular polarization (RHCP). In addition, RHCP is dominant over LHCP by > -20 dB at the same 5 GHz. This reveals that the proposed monopole antenna is an RHCP. So, gain and relative power of radiation pattern make it possible to identify the CP components in terms of LHCP or RHCP, actually a part of CEM (computational electromagnetics). The entire entity is represented in terms of horizontal components (x) and vertical components (y) through the characteristic mode theory (CMT) in Figure 5 which is deduced in Equation (4) and Equation (5) in a generalized manner which is further responsible for evaluating the far-field properties.

$$\vec{E}_{RHCP}(0,t) = E_0\cos(\omega t)\hat{x} + E_0\cos\left(\omega t + \frac{\pi}{2}\right)\hat{y} \tag{3}$$

The authors through the aforementioned analysis share the insights about the CP for proposed antenna that is based on CEM objectives at the same time and has satisfied the theoretical aspects. Thus, in this section, not only the concepts are explained on the basis of EM simulations, simultaneously its mathematical insights are also covered. So, by looking at the characteristics of CP and how it works, we can come up with the plan for large-scale solution. It is done to deal with sub-6 GHz 5G applications, which is the important task force for assessing, developing, and optimizing, especially for printed antennas that show CP features. To the best of the authors' knowledge, techniques I to III, parts of CEM, are a significant and infrequently described step that can be significantly used in our analysis for understanding the peculiarities of CP to a large extent.

$$\vec{E}_{LHCP} = \frac{1}{\sqrt{2}}\left(\vec{E}_x + j\vec{E}_y\right) \tag{4}$$

$$\vec{E}_{RHCP} = \frac{1}{\sqrt{2}}\left(\vec{E}_x - j\vec{E}_y\right) \tag{5}$$

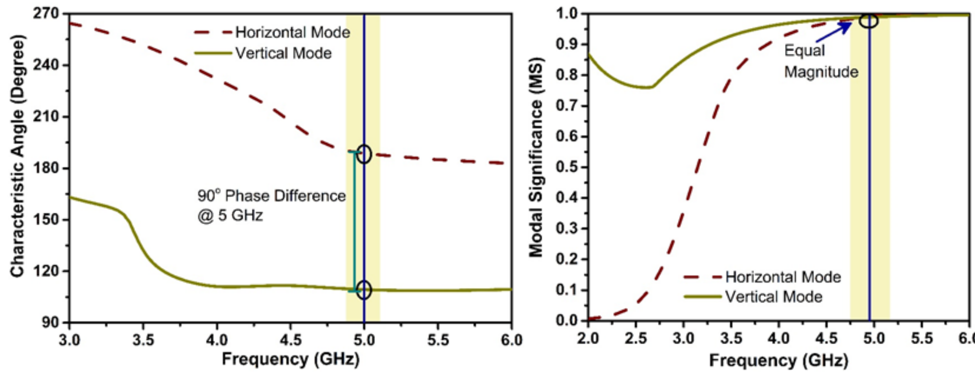

FIGURE 5. Evaluation of horizontal and vertical modes at 5 GHz through characteristic mode theory (CMT).

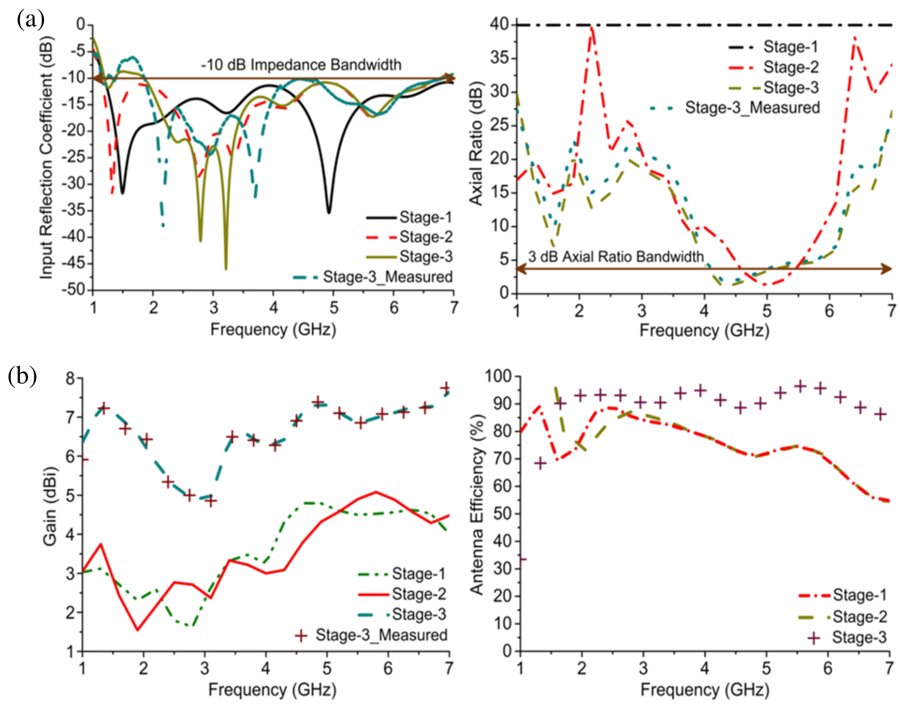

FIGURE 6. (a) Impedance bandwidth (10-dB BW) and (b) Axial bandwidth (3-dB BW) of SADEA-tuned CP MTS antenna.

4. EXPERIMENTAL VALIDATION WITH ITS RELEVANT OUTCOMES

Figures 1(a)–(c) present various characteristics of the proposed monopole antenna like developmental stages, final schematics, and its fabricated prototypes (front view, bottom view, & prospective view) by utilizing the concept of printed circuit board (PCB) prototyping mechanism. Then, Figure 6(a) shows the 10-dB impedance bandwidth (BW) for simulated and measured scenarios. Hence, the outputs for these two cases are 117.2% at 1.82–6.98 GHz with the bandwidth of 5.16 GHz and 116.3% at 1.84–6.96 GHz with bandwidth of 5.12 GHz. Similarly, the measured and simulated 3-dB axial bandwidths are 4.05–5 GHz, 0.95 GHz, with bandwidth of 20.98%, and 4.03–5 GHz, 0.97 GHz, with bandwidth of 21.52%. It offers the CP gain ranging from 5.5 to 7.9 dBic and antenna efficiency of > 85% in the operating frequency spectrum (sub-6 GHz 5G bands) as shown in Figure 6(b).

Certain factors are responsible for the advancement in antenna performance above traditional design, and the investigations are ongoing to uncover it. The increase in CP gain is achieved to a factor of 3.19 times, which is quite good to the best of the authors' knowledge in this particular area along with broadband 3-dB BWs. It is because of the improved impedance matching and reduced backscattering that contribute to the attainment of such increment. Prior to it, MTS is also known for influencing EM waves [16]. So, it is also responsible for enhancing the efficiency with which energies are concentrated in their required direction, and further it is equally responsible for reducing the sidelobes that contribute to the optimization of the spatial distribution of the energy radiated by RF front-ends. A strong directional pattern is provided by the radiation pattern at 5 GHz, which has a front-to-back ratio (FBR) > -22.5 dBic. Figures 7(a) through (c) illustrate a number of features associated with far-field radiation pattern right from measurement

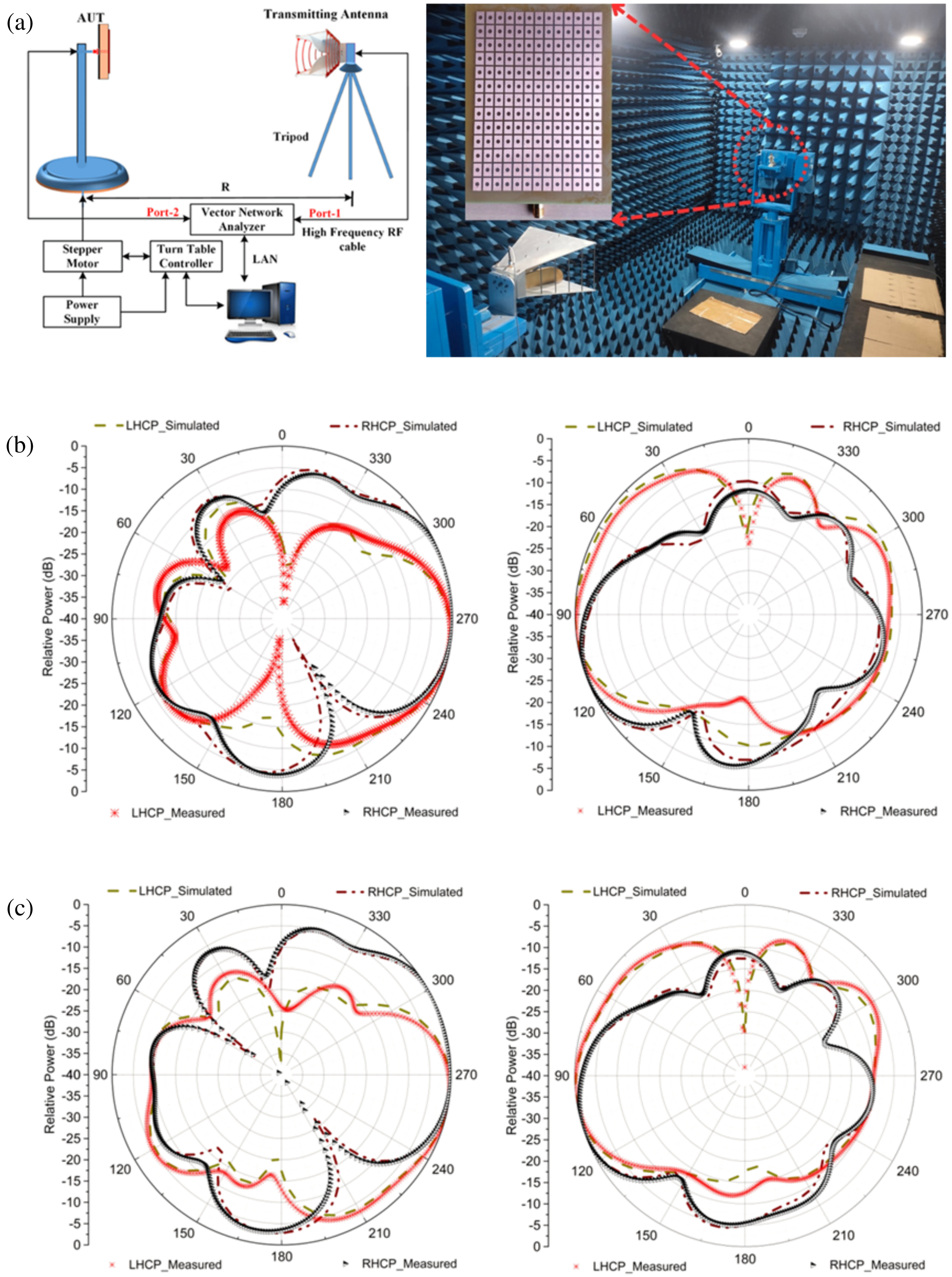

FIGURE 7. (a) Setup in the anechoic chamber, (b) Phi = 0°, & (c) Phi = 90° at 5 GHz of SADEA-tuned CP MTS antenna.

setup to its outcomes. The comparison with those reported in [5–12] is included in Table 3, w.r.t. performance trade-offs. The evidence indicates that the proposed antenna (stage-3) is superior to others, due to its higher bandwidths and enhanced CP gain. Finally, it achieves a CP peak gain > 7.28 dBic, addressing the constraint of conventional printed monopole antennas often characterized by low gain in their operating bandwidth.

5. UNDERSTANDING OF TIME-DOMAIN ANALYSIS W.R.T. NEXT-GENERATION WIRELESS APPLICATIONS

As a fundamental entity, time domain analysis is essential for broadband antennas. This analysis specifies capabilities of the signal transmission and reception with the least amount of dis-

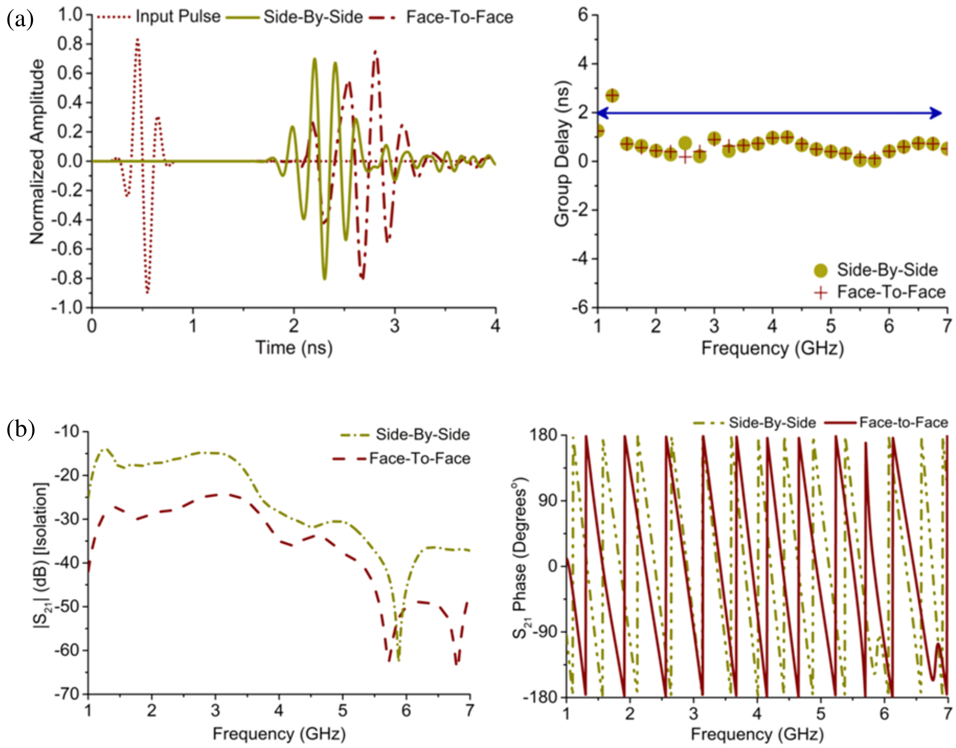

FIGURE 8. (a) Input signal & group delay and (b) S_{21} (isolation) at 5 GHz of the proposed antenna (stage-3).

tortion as possible in the communication channel. Over the right frequency ranges (below 7 GHz), the antenna's features are carefully checked such as group delay and isolation. We utilize CST microwave studio as an EM solver for evaluating time domain analysis. During it, we keep the proposed SADEA-tuned CP MTS antenna's (stage-3) identical radiating structures in two different positions: (a) side-by-side and (b) face-to-face, with 30 cm of free space in between each other. It is important to note that the monopole radiator is described in the broadside direction since this angle provides favorable outlook in terms of performance. So, the information presented in Figures 8(a) and (b) includes a comprehensive analysis as well as the results that correlate to it, especially with its signalling properties. When analyzing the properties of the signal's behaviour, a Gaussian pulse is of great use and is applied as the input signal. So, these findings reveal that communication systems require excellent pulse handling capability which is verified by good group delay and better isolation features. Since the proposed CP MTS antenna (stage-3) has a higher isolation greater than -25 dB and the linear phase fluctuation at sub-6 GHz 5G bands, a significant example is presented in the era of next-generation wireless applications.

The RF front end (antenna) is considered as a vital component of the RF energy harvesting and wireless power transmission system. In sub-6 GHz 5G bands, various ambient sources release the RF signals that the RF front end primarily receives. Hence, it is the reason that CP antennas facing the broadside direction and having a high CP gain are better, as the available RF energy in the surrounding environment can exist in any orientation and phase alignment. So, it is possible to combine indoor evaluations, which are linked to the Friis Transmission Equation and the outcomes that come from time domain analysis, an advantage for next-generation wireless applications.

6. CONCLUSION

This article looks into the proposed CP front-end with high gain that is supported by SADEA-Tuned Smart Metasurface (STSM) layer as a superstrate tuned to the AI-driven SADEA optimization method. Due to this, it is feasible to attain enhanced 10-dB BW and 3-dB BW, along with the peak gain of > 7.28 dBic and the antenna efficiency of $> 85\%$ in the bands allocated for its operation, i.e., in sub-6 GHz 5G bands. Here, we provide not only scientific insights about the CP, but also its intuition based on the CEM. So, we present a comprehensive plan to address the challenge of analyzing CP using MTS antennas (stage-3). Then, the findings achieved are compared with performance trade-offs. The growing needs of modern applications, which require communication at sub-6 GHz 5G bands, are paving a way towards the Reconfigurable Intelligent Surfaces (RISs) and unmanned aerial vehicles (UAVs). Further, our research concentrates on the Designing, Analyzing, Validating, and Implementing (DAVI) process, encompassing the stages such as designing, analyzing, validating, and implementing, enhancing its effectiveness. The future of sustainable energy harvesting technology will probably depend on the STSM as wireless communication networks expand, and the demand for low-power energy-efficient devices rises vital for the next-generation wireless applications.

REFERENCES

[1] Alsharif, M. H., R. Nordin, N. F. Abdullah, and A. H. Kelechi, "How to make key 5G wireless technologies environmental friendly: A review," *Transactions on Emerging Telecommunications Technologies*, Vol. 29, No. 1, e3254, 2018.

[2] Chen, Z. N., X. Qing, W. Liu, H. Sheng, T. Li, and B. Zhang, "Toward metantennas: Metasurface antennas shaping wireless communications," *IEEE Communications Magazine*, Vol. 62, No. 8, 94–99, 2024.

[3] Javanshir, A. M., T. Aribi, T. Sedghi, and A. Kalami, "High performance and compact antenna with new scheme for broadband circular polarisation applications," *International Journal of Electronics Letters*, Vol. 13, No. 1, 35–46, 2025.

[4] Meher, P. R. and S. K. Mishra, "Design and development of mathematical equivalent circuit model of broadband circularly polarized semi-annular ring shaped monopole antenna," *Progress In Electromagnetics Research C*, Vol. 129, 73–87, 2023.

[5] Elahi, M., A. Altaf, Y. Yang, K.-Y. Lee, and K. C. Hwang, "Circularly polarized dielectric resonator antenna with two annular vias," *IEEE Access*, Vol. 9, 41 123–41 128, 2021.

[6] Ameen, M. and R. Chaudhary, "Metamaterial circularly polarized antennas: Integrating an epsilon negative transmission line and single split ring-type resonator," *IEEE Antennas and Propagation Magazine*, Vol. 63, No. 4, 60–77, 2021.

[7] Tran, H. H., C. D. Bui, N. Nguyen-Trong, and T. K. Nguyen, "A wideband non-uniform metasurface-based circularly polarized reconfigurable antenna," *IEEE Access*, Vol. 9, 42 325–42 332, 2021.

[8] Dong, J., R. Wu, X. Yuan, and J. Mo, "A low-profile broadband circularly polarized metasurface antenna based on characteristic mode analysis," *Waves in Random and Complex Media*, Vol. 35, No. 2, 2411–2429, 2025.

[9] Chi, Y., "A new wideband CP antenna with a single-layer metasurface," *Electromagnetics*, Vol. 42, No. 8, 616–623, 2022.

[10] Chai, K., Z. Li, Y. Zhao, L. Han, G. Han, and Y. Liu, "A low-profile wideband circularly polarized metasurface antenna based on characteristic mode analysis," *International Journal of Microwave and Wireless Technologies*, Vol. 16, No. 2, 244–251, 2024.

[11] Rana, S. and P. Jain, "Utilizing characteristics mode analysis for designing a miniaturised high-gain metasurface antenna with wideband circular polarization and reduced scattering," *Journal of Electromagnetic Waves and Applications*, Vol. 38, No. 8, 842–859, Apr. 2024.

[12] Pang, H., J. Zhao, and J. Xu, "Miniaturized circularly polarized metasurface antenna based on characteristic mode analysis," *Microwave and Optical Technology Letters*, Vol. 66, No. 1, e33983, 2024.

[13] Liu, B., H. Aliakbarian, Z. Ma, G. A. E. Vandenbosch, G. Gielen, and P. Excell, "An efficient method for antenna design optimization based on evolutionary computation and machine learning techniques," *IEEE Transactions on Antennas and Propagation*, Vol. 62, No. 1, 7–18, 2014.

[14] Liu, B., S. Koziel, and N. Ali, "SADEA-II: A generalized method for efficient global optimization of antenna design," *Journal of Computational Design and Engineering*, Vol. 4, No. 2, 86–97, 2017.

[15] Liu, Y., B. Liu, M. Ur-Rehman, M. A. Imran, M. O. Akinsolu, P. Excell, and Q. Hua, "An efficient method for antenna design based on a self-adaptive bayesian neural network-assisted global optimization technique," *IEEE Transactions on Antennas and Propagation*, Vol. 70, No. 12, 11 375–11 388, 2022.

[16] Behera, B., S. Mishra, M. H. Alsharif, P. Uthansakul, and M. Uthansakul, "A metasurface-inspired printed monopole antenna for 5G and RF energy harvesting application," *Engineering Science and Technology, An International Journal*, Vol. 51, 101638, 2024.